THE ANTENNA LABORATORY

GPO PRICE $ ______

CFSTI PRICE(S) $ ______

Hard copy (HC) 2.00

Microfiche (MF) .50

ff 653 July 65

RESEARCH ACTIVITIES in ---

Automatic Controls *Antennas* *Ech*
Microwave Circuits *Astronautics* *E M*
Terrain Investigations *Radomes* *Syste*
Wave Propagation *Sub*

FACILITY FORM 602

~~N66-13141~~ (ACCESSION NUMBER)	(THRU)
28 (PAGES)	/ (CODE)
CR 68549 (NASA CR OR TMX OR AD NUMBER)	29 (CATEGORY)

Observations Made of Submillimeter-Wavelength Solar Radiation Using the McMath Solar Telescope of The Kitt Peak National Observatory

R. A. Williams

Grant Number NsG-74-60

1093-27

13 August 1965

Prepared for:
National Aeronautics and Space Administration
Office of Grants and Research Contracts
Washington, D. C. 20546

Department of ELECTRICAL ENGINEERING

THE OHIO STATE UNIVERSITY
RESEARCH FOUNDATION
Columbus, Ohio

NOTICES

REPORT 1093-27

REPORT

by

THE OHIO STATE UNIVERSITY RESEARCH FOUNDATION
COLUMBUS, OHIO 43212

Sponsor	National Aeronautics and Space Administration Office of Grants and Research Contracts Washington, D. C. 20546
Grant Number	NsG-74-60
Investigation of	Receiver Techniques and Detectors for Use at Millimeter and Submillimeter Wave Lengths
Subject of Report	Observations Made of Submillimeter-Wavelength Solar Radiation Using the McMath Solar Telescope of the Kitt Peak National Observatory
Submitted by	R. A. Williams Antenna Laboratory Department of Electrical Engineering
Date	13 August 1965

ABSTRACT

13141

Solar radiation measurements in the region from 60 microns to one millimeter wavelength were conducted during April 1965 at Kitt Peak National Observatory near Tucson, Arizona. The manner in which these tests were conducted and the results obtained are described in this report. It was found that when the total precipitable water-vapor content in the atmospheric path from the sun to the telescope was less than about 0.2 centimeters solar radiation was observed at several atmospheric windows having wavelengths greater than 300 microns, with the maximum transmission through the window at 345 microns wavelength being on the order of two percent. The spectral data obtained under a variety of total water-vapor columns and path lengths are presented in a series of charts contained within this report.

Author

TABLE OF CONTENTS

OBSERVATIONS MADE OF SUBMILLIMETER-WAVELENGTH SOLAR RADIATION USING THE MCMATH SOLAR TELESCOPE OF THE KITT PEAK NATIONAL OBSERVATORY

INTRODUCTION

The submillimeter-wavelength solar-radiation spectrum was measured during April 1965 at the Kitt Peak National Observatory which is located about fifty miles west of Tucson, Arizona. One of the auxillary heliostats of the McMath Solar Telescope was used as the collecting system, and a Michelson-type interference spectrometer and a helium-cooled germanium bolometer were used to measure the incoming radiation. The interference spectrometer idea was first used by Peter Fellgett in 1951[1, 2] and has since been used by numerous experimenters, including H. A. Gebbie who used it in 1957 to obtain a measurement of the solar spectrum over a portion of the submillimeter region from the Jungfraujoch in Switzerland[3]. Some of the aspects of submillimeter wavelength radiometry were presented at the Orlando Millimeter and Submillimeter Conference in 1963[4] and the present instrument was described in a paper presented at the Polytechnic Institute of Brooklyn's Symposium on Quasi-Optics in June, 1964 [5]. Therefore, the present paper will deal primarily with the actual measurements conducted at the Kitt Peak Observatory.

EXPERIMENTAL EQUIPMENT

Figure 1 shows the basic instrument operating principle. The incoming radiation is chopped by a Pyrex glass chopper which effectively totally chops the incoming submillimeter and far-infrared radiation, but only slightly chops the near-infrared and visible radiation. A black polyethelene filter placed after the chopper then removes the near-infrared and visible radiation but allows the far-infrared and submillimeter-wavelength radiation to pass on through to the interferometer and the radiation detector. Re-radiation from the black polyethelene filter does not contribute to the output signal from the radiation detector because of the filter's location following, rather than preceding, the chopper (the filter was also tried at a location just ahead of the radiation detector, but it was then found that heating of the interferometer beam splitter material by the near-infrared and visible solar radiation caused it to distort slightly). Effectively the radiometer is a Dicke-type system in the submillimeter and far-infrared regions where the chopper blade material is a good absorber, the temperature of the chopper blade corresponding to the Dicke-system matched-load temperature. The chopper blade was artificially heated by a strong incandescent lamp bulb so as to maintain it at a relatively constant temperature regardless of whether solar radiation was or was not present in the input radiation.

The interferometer has been described in an earlier paper [5] and consists of a wire-mesh beam splitter, a fixed mirror, and a movable mirror whose position is slowly shifted from the "white light" position, where the path length from the beam splitter to and from each of the mirrors is equal, to a position where the path length to and from the movable mirror is γ_{max} centimeters longer than the path length to and from the fixed mirror. The magnitude of the radiation detector signal is obtained and recorded as a function of the path-length difference γ, and this function is referred to as an "interferogram". Taking the inverse cosine Fourier transform of the interferogram function yields an approximation to the radiation spectrum, the actual result being a function which is obtained from the convolution of the actual radiation spectrum reaching the detector with an instrument response function which is shown in Fig. 2. The instrument response function is similar to the passband function of any radio or microwave receiver except that it has a number of side lobes, some of which are negative. The bandwidth of the response function which is defined as $(\Delta\nu)$ in Fig. 2 is equal to $1/\gamma_{max}$ where γ_{max} is the maximum value of the path length difference (twice the maximum amount the movable mirror is moved). The spectral results obtained are also modified by the transmission and absorption characteristics of the chopper blade and the black polyethelene filter, by the beam splitter efficiency curve, and by the radiation-detector response curve. Noise will also be present on the measured spectrum due to noise in the radiation detector and the electronic system, and also due to any variations which occur in the source output or in the attenuation in the atmospheric path between the source and the radiation detector during the time that the test is being conducted. Since attempting to improve the instrument resolution by narrowing the instrument response function (decreasing $(\Delta\nu)$ by increasing γ_{max}) leads to a smaller signal-to-noise ratio, one is limited in the degree to which the spectrum may be resolved. When making solar radiation measurements in the submillimeter region the low signal levels due to the great amount of atmospheric absorption and the large amount of noise introduced by the fluctuations in the level of this absorption severely limit the resolution which may be obtained.

The measurements at Kitt Peak Observatory were made by using an unfocused beam of light from the 24-inch East Auxillary heliostat. A 12-inch diameter portion of this beam was concentrated into a 3-inch diameter collimated beam through the use of a 12-inch spherical mirror, a small aluminum flat, and a 3-inch off-axis parabolic mirror. Figure 3 is an outside view of the McMath Solar Telescope showing the heliostat mirrors at the top of the tower and showing the sloping polar-axis tunnel through which the solar beam is directed to an observing room located inside of the mountain. Figure 4 shows the interferometric radiometer as set up inside of the observing room. The 12-inch spherical mirror is at the right foreground and the aluminum flat, chopper, and the 3-inch parabolic mirror are shown mounted on the plywood table. Behind the 3-inch mirror is the black polyethelene filter and behind it is the beam splitter and the interferometer mirrors. The Texas Instruments helium-cooled gallium-doped germanium bolometer which was used as the radiation detector is to the right of the beam splitter.

The solar radiation from the heliostat mirror traveled about 150 feet down the inside of the polar-axis tunnel and then about fifty feet through the observing-room atmosphere before finally reaching the radiation detector. Although the walls of the polar tunnel are maintained at about 40 degrees Farenheit the temperature of the air in the tunnel varied somewhat from this figure. The observing-room temperature varied between 60 and 66 degrees Farenheit.

The data obtained from the observations was recorded in digital form on punched paper tape and was processed and plotted by the IBM 7094 and 1620 computers at The Ohio State University. Weather observations of temperature, cloud cover, and the total precipitable water vapor were recorded during each observation. An instrument constructed by Dr. Frank J. Low of the University of Arizona and the National Radio Observatory was used to measure the total amount of precipitable water vapor in the atmospheric path between the sun and the telescope site. This instrument works on the principle of comparing the intensity of the received solar radiation within and just outside of a water vapor absorption band in the near infrared.

DETERMINATION OF ATMOSPHERIC WINDOWS

In the submillimeter and far-infrared regions the absorption of radiation by the atmosphere is quite severe. At high humidities an appreciable attenuation is obtained over a path length of just a few feet. The few atmospheric windows which do exist in this region are "windows" only in the sense that under the right conditions some small amount of radiation may get through. The Kitt Peak measurements were made by observing radiation from both the sun and the sky under a number of different humidity and path-elevation angles. By comparing solar-radiation and sky-radiation measurements obtained under the same approximate conditions one can determine where spectral windows exist and obtain some estimate of their magnitude. In Fig. 5 are shown the spectral results which might be obtained under several different conditions of window clarity. The solid line represents the measurements obtained when observing solar radiation and the dotted line represents the sky-radiation measurements. In (a) it is assumed that the absorption is so complete that no signal from the radiation chopper gets through the two-meter long path between it and the detector, while in (b) the attenuation is somewhat less and a signal is present due to the difference between the temperature of the chopper blade and that of the room air which is now acting as a black body source. However, the attenuation over the path length in the room atmosphere still prevents any solar radiation or radiation from the outside air from reaching the instrument. In (c) the window is a little clearer and the room path is partially transmitting so that some radiation from the outside air is reaching the instrument. In general, the clearer the window the deeper the dip in the dotted line will be, since the higher, colder layers of the atmosphere will be acting as the source and the attenuation over the room path and the lower, warmer atmospheric layers will be less. It is assumed in (c) that only a very small amount of solar radiation is penetrating the atmosphere and therefore the solid line departs only slightly from the dotted line. In a practical experiment this difference might be masked by the noise level on the results. In (d) it is now assumed that the center of the window is clear enough so as to allow some measurable amount of solar radiation to penetrate the atmosphere and the solid line departs considerably from the dotted line and has a positive peak. At the same time the measurement made of the sky radiation (dotted line) should show a deeper dip than in (c) since at least a portion of the radiation being received will have its origin outside of the earth's atmosphere and this source will presumably be much colder than the atmosphere itself. In other words, although some radiation is still being received from the earth's atmosphere, the atmosphere can no longer be considered as a "black" body, but only as a "gray" body radiator.

These then are the results which one would expect to obtain from comparative measurements of the sky and solar radiation with a noiseless Dicke-type radiometer of infinitely small bandwidth whose matched load was kept at a temperature somewhat above that of the room where it was located. In practice of course one must contend with a finite signal-to-noise ratio and an instrument response function of finite bandwidth and non-ideal shape (such as the $(\sin x)/x$ form of the interference spectrometer's response function shown in Fig. 2).

EXPERIMENTAL RESULTS

Because of a large amount of very poor to only fair observing weather during most of the period during which observations were conducted at Kitt Peak the results which could be obtained are somewhat limited. However, there were a couple of days when conditions could be classed as "good" and some very interesting results were obtained from these data. Inasmuch as the total precipitable water-vapor column never did fall as low as one millimeter, none of the observing time could be classed as "excellent". Most of the time the water-vapor column was in the vicinity of $2\text{-}\frac{1}{2}$ to $3\text{-}\frac{1}{2}$ millimeters or greater.

In general the following conclusions can be drawn from the results obtained:

(A). At less than two millimeters of precipitable water vapor measurable amounts of solar radiation are observed at several wavelengths longer than 300 microns while a few lesser windows are indicated at shorter wavelengths. However, even the clearest windows are still relatively opaque in terms of the total amount of solar energy transmitted.

(B). With from two to four millimeters of water vapor some solar radiation is still indicated, although the level of radiation is approaching the noise level of the instrument, and

(C). At more than five millimeters of water vapor the solar radiation signal completely disappears into the noise level.

Specific results are presented in Charts I through VII, the first five charts covering the region up to approximately 110 wavenumbers (about 90 microns wavelength) and representing results obtained with a 200 line-per-inch nickle mesh used as the beam splitter. Charts VI and VII cover the region from approximately 60 to 163 wavenumbers (about 165 to 62 microns wavelength) and represent data taken using a 500 line-per-inch mesh beam splitter. The conditions under which the various tests were run are indicated in Table I. Unless noted by the comment "low resolution" the tests were conducted and processed so as to give an instrument response function having a central-peak bandwidth, $(\Delta\nu)$, (see Fig. 2) of 0.642 wavenumber units (cm^{-1}). This was obtained by allowing the path-length difference, Y, to change from 0 to 1.56 centimeters over a period of 105 minutes. In some cases it was not possible to obtain an undisturbed signal for this length of time (due to the passage of clouds or the occurrence of other unpredicted events) or else it was found advantageous from the standpoint of improved signal-to-noise ratio to process the interferogram data only to a path length difference of 0.78 centimeters, resulting in an instrument resolution of $(\Delta\nu)$ = 1.284 wavenumbers. These tests are noted in Table I as "low resolution" tests. In preparing Charts I through VII it was attempted to in each case match a solar radiation test and a sky radiation test taken under similar conditions.

Chart XIII represents the results obtained when a black-body source at 100 degrees Celsius is put at the focus of the three-inch parabolic mirror. Under these conditions the total path length from the source to the radiation detector is about two meters. The total precipitable water vapor in this path during the test was approximately 5.5×10^{-4} centimeter. However, due to the low source temperature little signal was obtained at wavelengths longer than about 350 microns. The peaking in the 190 to 350 micron region is due to peaking of the beam-splitter efficiency in this region as well as the effects of the black polyethelene and crystal quartz filters and detectors windows which begin to attenuate below about 90 microns wavelength.

Beginning with Chart I it is seen that a number of definite windows occur at wavelengths longer than 300 microns. Due to the poor relative resolution of the instrument at the longer wavelengths the test results indicate good transmission of the atmosphere at all wavelengths longer than about 0.9 millimeter. Major window areas are indicated centered at about 810, 710, 590, 440, and 345 microns wavelength. These regions are marked by solid bars at the bottom of the chart. At wavelengths shorter than 300 microns a number of partial atmospheric windows are indicated as shown by dips in both the solar radiation and sky radiation curves. These regions have been marked by dotted bars at the bottom of the chart. Because of the relatively large noise level on the input data and the large side lobes which occur on either side of the main peak of the instrument response function (which will give a substantial reverse-polarity signal on either side of the area where a narrow window occurs) some care must be taken in interpreting the data in Charts I through VII. Chart VIII is of some help in differentiating true atmospheric windows from apparent ones which are caused by noise or the instrument response function side lobes. Any apparent windows or Charts I through VII which fall within absorption bands on Chart VIII are marked by question marks. It will be noted that at wavelengths shorter than 300 microns in Chart I that the solar-radiation test apparently indicates a temperature lower than does the sky-radiation test at many points. Part of this discrepancy is due to the chopper blade operating about two to three degrees Celsius warmer during a solar test than during a sky-radiation test, and part may be due to a difference in the atmospheric conditions under which the two tests were conducted.

The most prominent window occurs around 345 microns wavelength and by calibrating the instrument with a black-body source it was estimated that this peak represented a temperature about 75 degrees Celsius warmer than the chopper blade temperature (25 degrees C) or roughly about 373 degrees Kelvin. Similarly, the sky radiation measurement indicates an effective temperature about 22 degrees less than that of the chopper blade during the sky radiation measurement ($22\frac{1}{2}$ degrees C) or approximately 273 degrees Kelvin. Thus, the total apparent temperature change due to the presence or absence of the solar radiation is of the order of 100 degrees Kelvin. Assuming that the sun is a black body radiator at these wavelengths, one would, in the absence of any atmospheric attenuation, expect to measure a temperature difference of about 6000 degrees Kelvin between the solar radiation and the sky (space) radiation. From these results one can conclude that under the conditions of this test (a water-vapor column of about 1.7 millimeters) that the maximum atmospheric transmission in the 345-micron window is only about 100/6000 or about 1.7 percent. In general the window positions on Chart I correlate fairly well with those published by H. A. Gebbie [3] whose experiment was conducted under similar conditions of total precipitable water vapor column.

Going to Chart II, where the solar radiation test was conducted under conditions of sixty to seventy percent greater water-vapor content and twice the instrument resolution, but with the same approximate path length through the atmosphere as on Chart I, one immediately notices that the transmission of radiation at wavelengths longer than 300 microns does not occur to near the extent to which it did under the conditions of the tests in Chart I. This is especially true of the 345 micron and 440 micron windows. The 590 micron, 710 micron and 810 micron windows are still present but of lesser magnitude as is the portion of the spectrum which is above 0.9 millimeter wavelength. The better instrument resolution and/or the increased absorption has split the windows originally centered around 440, 590, and 710 microns into two parts each and has put a couple of deep dips into the 810 micron window. The partial windows at wavelengths shorter than 300 microns do not show a marked change from Chart I to Chart II. This is probably due to the fact that one is still looking at about the same effective source temperature in both cases (i.e., some portion of the outside air) and also because the absorption along the path through the observing room stayed relatively constant from test-to-test (in the partial windows at wavelengths shorter than 300 microns most of the absorption appears to occur over the portion of the radiation path in the room while in the clearer windows at wavelengths longer than 300 microns most of the absorption appears to occur in the outside air).

Chart III is similar to Chart II except that the water vapor column on the solar test was slightly greater and the total path length through the atmosphere was somewhat less on the latter test. The results also appear to be somewhat noisier, possibly due to a greater amount of near-infrared and visible radiation being present. However, the fact that more submillimeter-wavelength radiation appears to be transmitted in the windows at wavelengths longer than 300 microns on Chart III than on Chart II suggests that the path length may have as much influence on the transmission as does the total amount of water vapor encountered along the path.

Chart IV is a low-resolution chart from tests made under the conditions of approximately the same path length but twice the water vapor content as the Chart I tests. It is interesting to compare this with Chart I and notice the gradual decrease in the relative window transmission from the 1 millimeter wavelength region where the transmission is comparable to that of Chart I to the region around 345 microns where a fairly good window occurring on Chart I becomes only a partial window (as indicated by a dip in both the sky and solar tests) on Chart IV.

Chart V shows a solar test made early in the morning with a somewhat greater total water-vapor column than the solar test on Chart II. Additional loss of signal in the windows at wavelengths greater than 300 microns is indicated.

Charts VI and VII show tests made using a 500 line-per-inch mesh beam splitter which has a peak efficiency in the vicinity of 85 to 95 microns. Chart VI represents results obtained with about 0. 24 cm of water vapor and Chart VII represents results obtained with from 0. 36 to 0. 5 cm of water vapor present during the respective solar tests. Although Chart VI shows several small windows occurring, it is questionable as to whether these are actually windows or just a combination of noise and the effects of the instrument response function side lobes. The only noticeable difference between the two charts is the absence of the apparent windows which occur on Chart VI but not on Chart VII and the slightly deeper dips in the partial windows on Chart VI than on Chart VII.

CONCLUSIONS

The absorption of radiation by atmospheric water vapor is quite severe in the submillimeter-wavelength region beyond 0. 9 millimeters wavelength. With a total precipitable water vapor column of about 0. 17 centimeter and with the sun approximately 30 degrees from the zenith the estimated transmission in the atmospheric window centered at 345 microns wavelength is about 1. 7 percent. Other windows which are indicated occur at 440, 590, 710, and 810 microns wavelength. Some of these apparently consists of two or more windows which blend together under this test condition, but appear as narrower, more opaque, separate windows when the water vapor content of the atmospheric path and/or the instrument resolution is greater. Increasing the total precipitable water vapor to more than 0. 3 centimeter greatly reduces the amount of radiation transmitted through the windows, and for all practical purposes the window at 345 microns disappears almost entirely. Even at 0. 17 centimeter of precipitable water vapor there are only partial windows which transmit no measurable amount of solar radiation at wavelengths shorter than 300 microns.

ACKNOWLEDGMENTS

The help and guidance of Dr. William S. C. Chang, formerly of The Ohio State University Antenna Laboratory and presently Chairman of the Electrical Engineering Department of Washington University, Saint Louis, Missouri, in helping to initiate and carry out this study are gratefully acknowledged, as are the excellent help and co-operation which were extended to the author by the personnel of Kitt Peak National Observatory during the period in which the observations described in this report were made. Particular thanks go to Dr. A. Keith Pierce, Director of the Solar Division of Kitt Peak Observatory, and his staff for helping to plan and conduct the observations.

REFERENCES

1. Fellgett, Peter, Doctorial thesis, Cambridge University (England), (1951).

2. Fellgett, Peter, "Spectrome'tre interfe'rentiel multiplex pour measures infra-rouges sur les e'toiles," J. Phys. et Rad., v19, 187 (1958).

3. Gebbie, H. A., "Detection of submillimeter solar radiation," Phys. Rev. (letter), v107, 1194 (1957).

4. Williams, R. A. and Chang, W. S. C., "Radiometry in the submillimeter region using the interferometric modulator," IEEE Transactions on MTT, vMTT-11, 513 (1963).

5. Williams, R. A. and Chang, W. S. C., "Interferometric wavelength selection for submillimeter radiometry," Polytechnic Institute of Brooklyn, Procd. of Symp. on Quasi-Optics, v14, 607 (1964).

TABLE I

TEST	INPUT RADIATION	BEAM SPLITTER	TIME (MST)	H_2O (cm.)	WEATHER AND NOTES
A	SOLAR RADIATION	200LPI	1040-1130	0.16-0.18	Warm, Low resol. test
B	SOLAR RADIATION	200LPI	1022-1208	0.24-0.3	Warm
C	SOLAR RADIATION	200LPI	1215-1400	apprx. 0.3	Warm
D	SOLAR RADIATION	200LPI	1450-1545	$>$ 0.32	Warm, Low resol. test
E	SOLAR RADIATION	200LPI	0832-1017	0.32-0.25	Warm
F	SKY (Decl = 32 deg and R.A. = 0 hrs)	200LPI	0820-1005	(0.21-0.17)*	Warm, Low resol. test
G	SKY (Decl = 32 deg and R.A. = 0 hrs)	200LPI	1400-1545	($<$ 0.27)*	Moderate temperature
H	SKY (Decl = 10 deg and R.A. = 0 hrs)	200LPI	0820-1005	(0.21-0.17)*	Warm
I	SKY (Decl = 10 deg and R.A. = +2½ hrs)	200LPI	1658-1843	($<$ 0.37)*	Warm, Low resol. test
J	SKY (Decl = 10 deg and R.A. = -4½ krs)	200LPI	0455-0550	($<$ 0.5)*	Cool
K	SOLAR RADIATION	500LPI	0930-1120	0.24	Cool
L	SOLAR RADIATION	500LPI	1448-1633	0.36 - 0.5	Warm
M	SKY (Decl = 8.5 deg and R.A. = +1 hr)	500LPI	1640-1735	($<$ 0.4)*	Cool, Low resol. test

*The water vapor content along the solar path during the same time period. Usually the water vapor content along the path over which the sky radiation measurement is being made will vary somewhat from this depending upon whether the solar path or the sky radiation path is longer (i.e. depending upon the respective elevation angles).

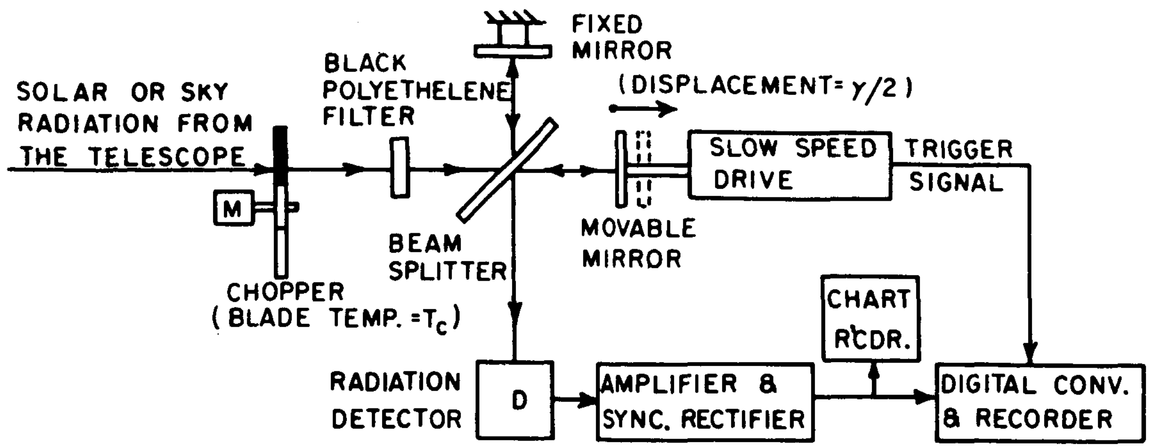

Fig. 1. A block diagram of the Dicke-type submillimeter interferometric radiometer receiver.

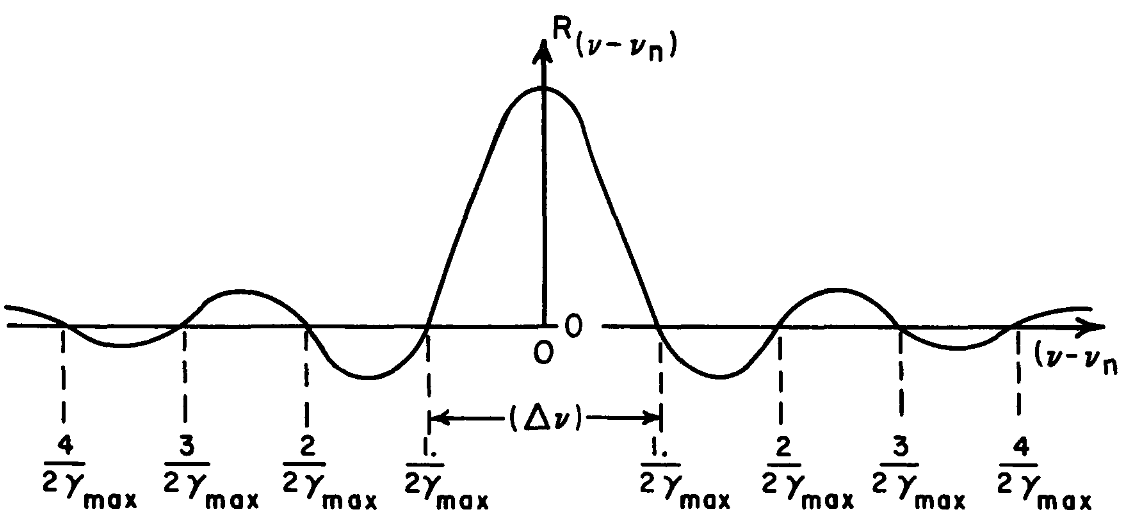

Fig. 2. The frequency response function of the interferometric receiver (or interference spectrometer as it is sometimes called). The bandwidth $(\Delta\nu)$ is defined as the wavenumber interval between the first response function zero crossing on either side of the main peak.

Fig. 3. The McMath Solar Telescope, Kitt Peak National Observatory, Arizona.

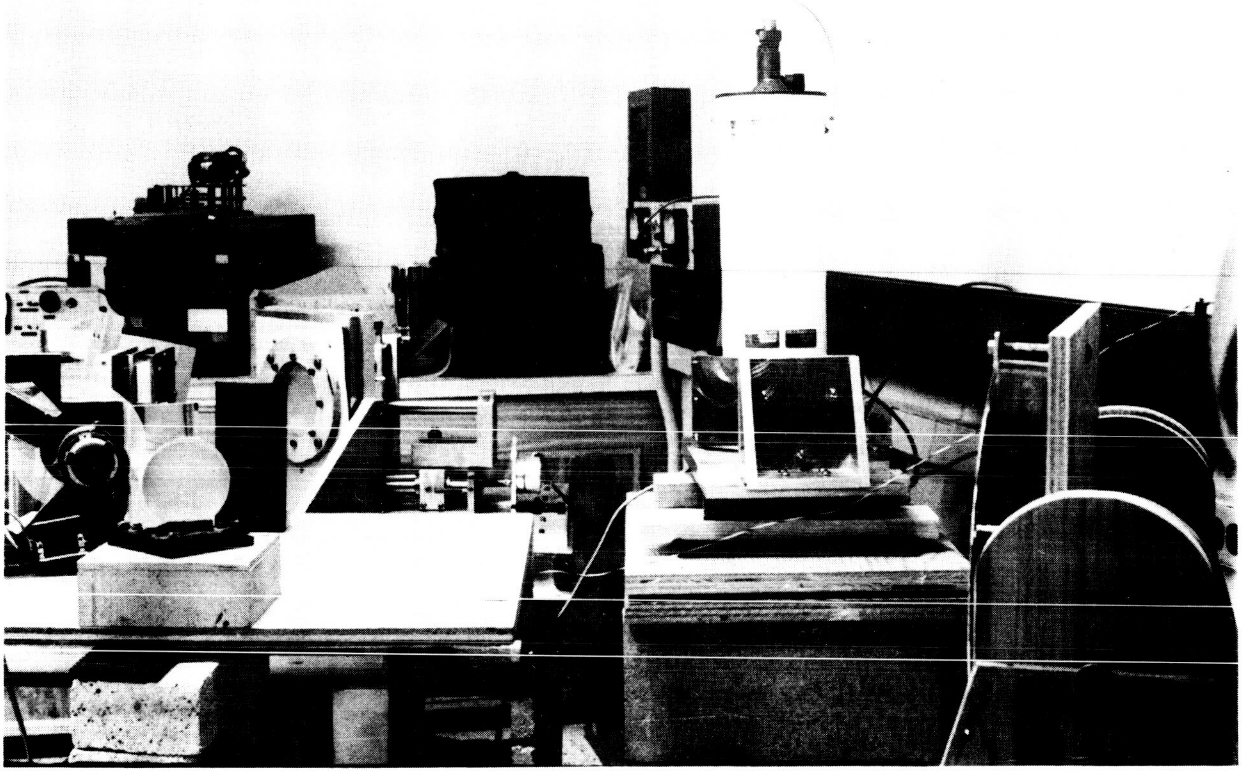

Fig. 4. The interferometric radiometer set up in the observing room of the McMath Solar Telescope.

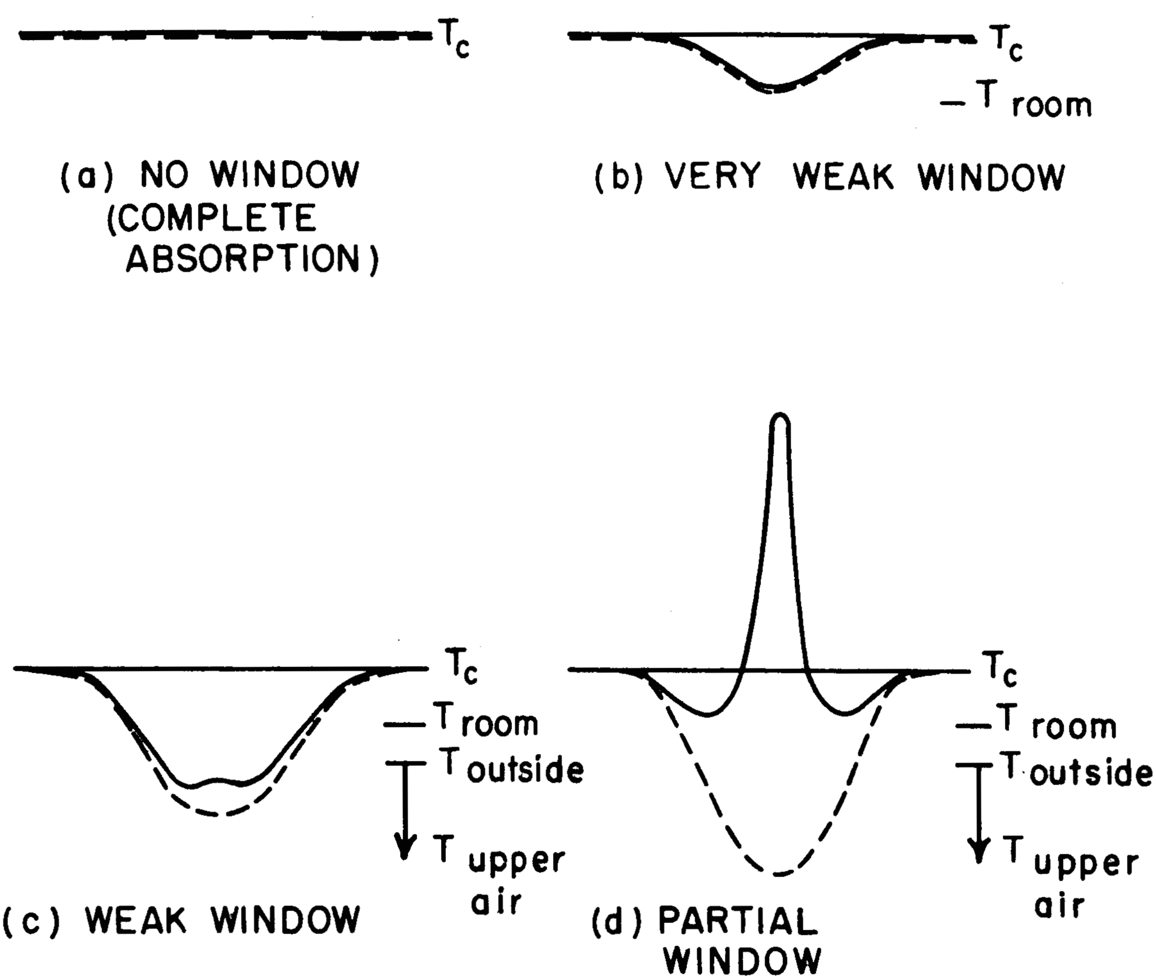

Fig. 5. The effects of various degrees of atmospheric window clarity upon comparative measurements of submillimeter-wavelength sky and solar radiation. The solid line represents a solar-radiation measurement and the dotted line a sky-radiation measurement. Positive temperature is plotted upward and the abscissa represents frequency (wavenumber). The zero axis represents the chopper blade temperature.

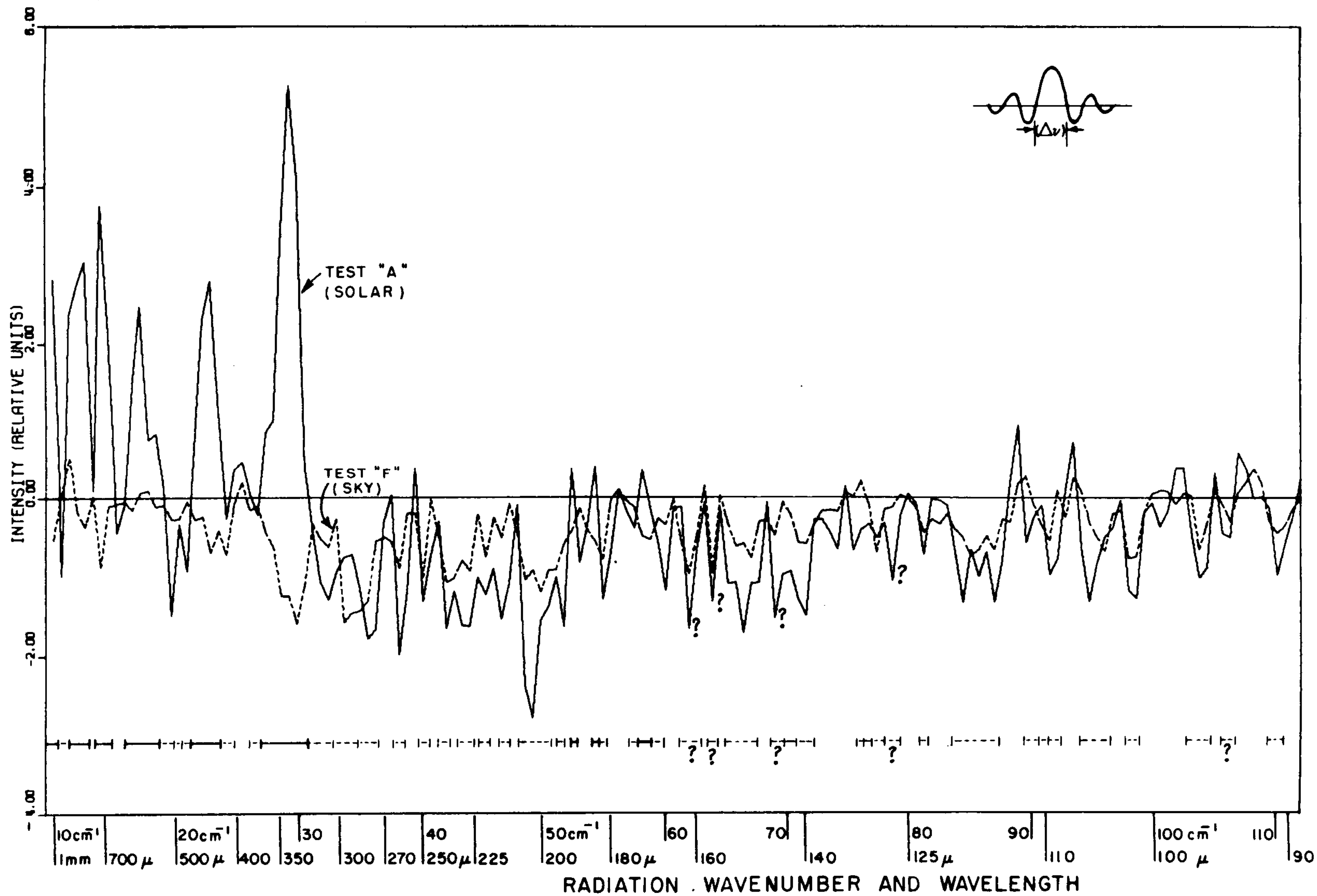
TEST "A" (SOLAR)
TEST "F" (SKY)
INTENSITY (RELATIVE UNITS)
6.00
4.00
2.00
0.00
-2.00
-4.00
10cm⁻¹ 1mm
700 μ
20cm⁻¹ 500 μ
400
350
30
300
270
40 250 μ
225
50cm⁻¹ 200
180 μ
60
160
70
140
80 125 μ
90
110
100 cm⁻¹ 100 μ
110
90
RADIATION . WAVENUMBER AND WAVELENGTH

Chart I

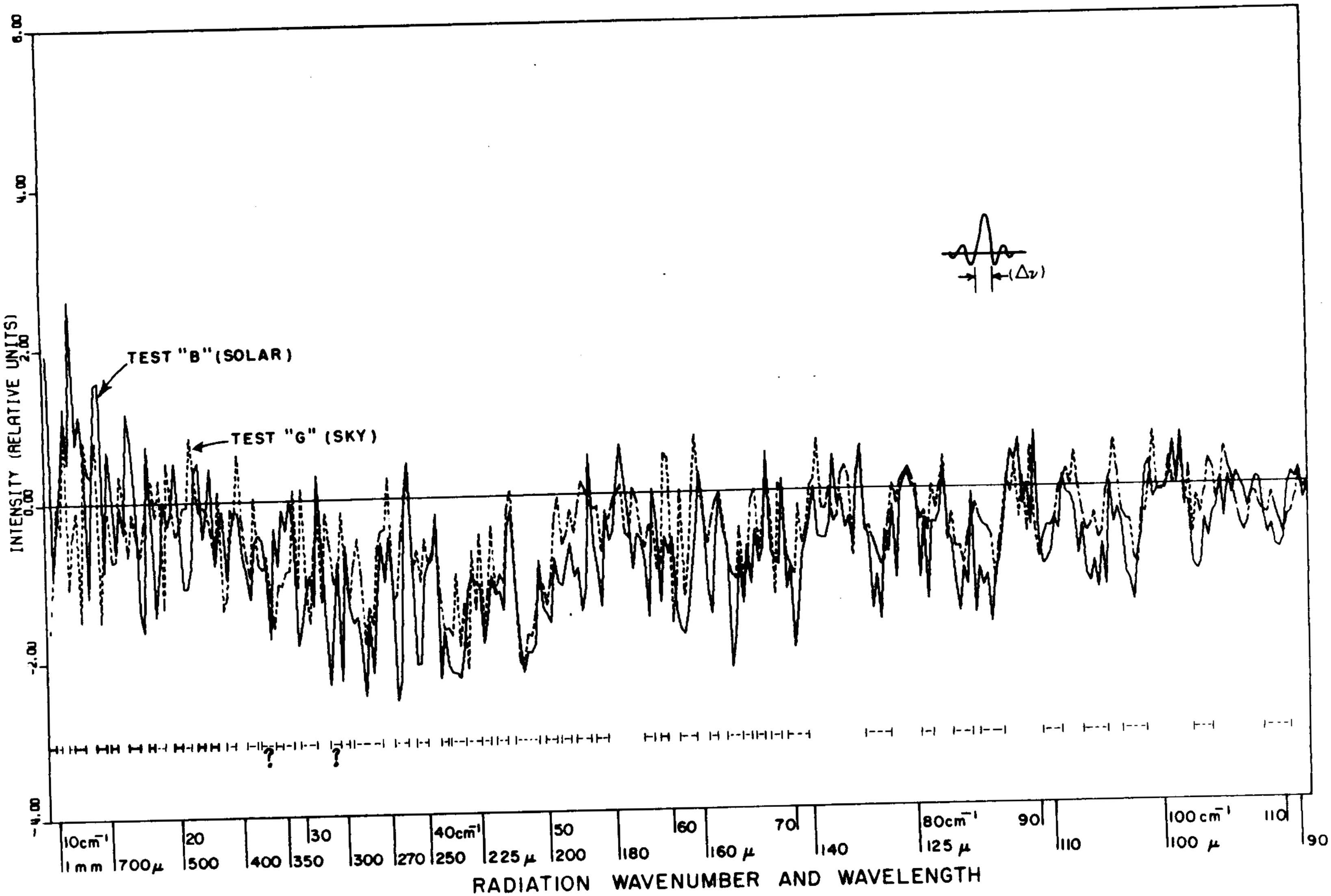
INTENSITY (RELATIVE UNITS)
6.00
4.00
2.00
0.00
-2.00
-4.00
TEST "B" (SOLAR)
TEST "G" (SKY)
(Δν)
10cm⁻¹
1 mm
700μ
20
500
400
30
350
300
270
40cm⁻¹
250
225μ
50
200
180
60
160μ
70
140
80cm⁻¹
125μ
90
110
100 cm⁻¹
100μ
110
90
RADIATION WAVENUMBER AND WAVELENGTH

Chart II

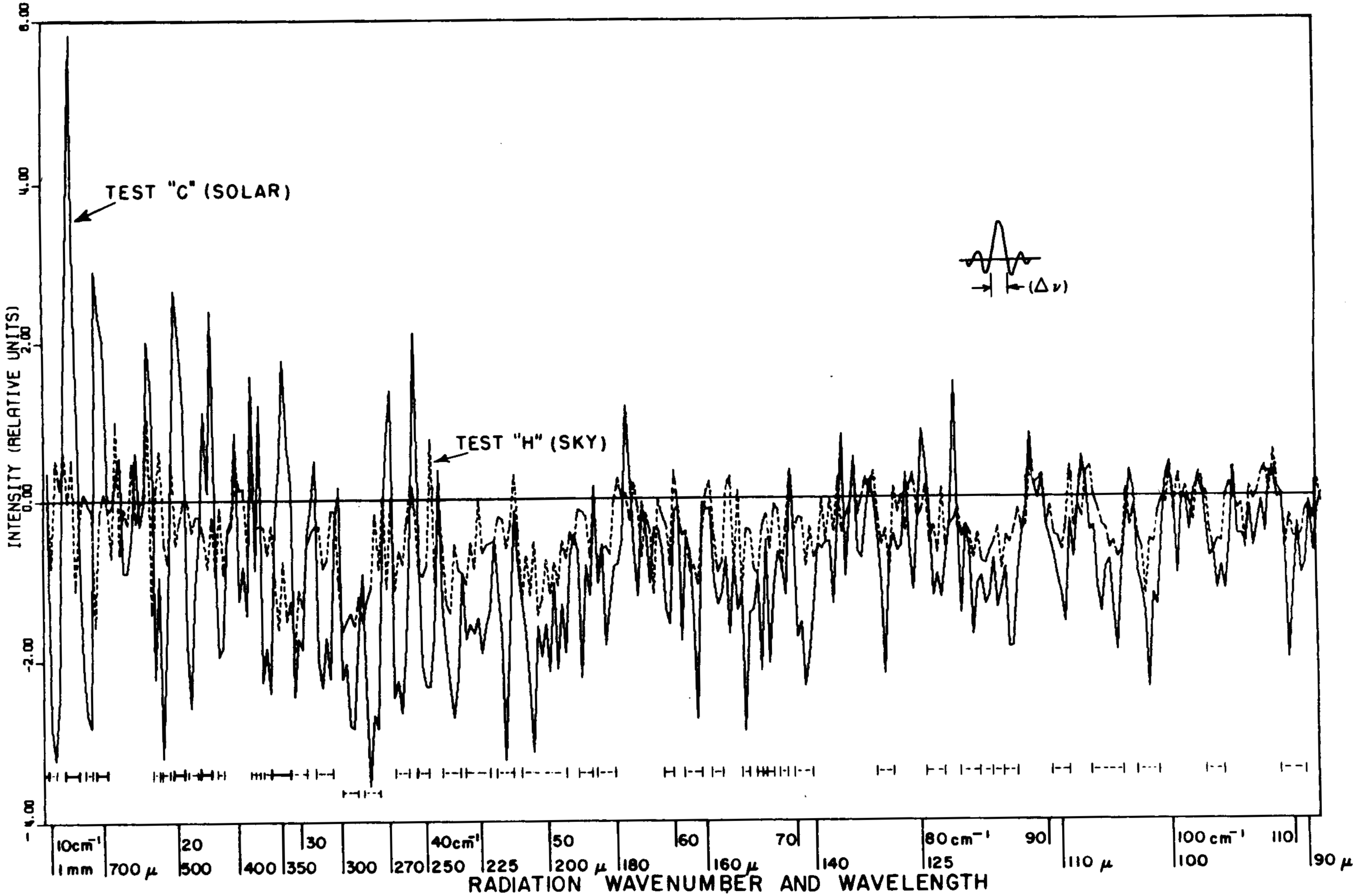

INTENSITY (RELATIVE UNITS)
6.00
4.00
2.00
0.00
-2.00
-4.00
TEST "C" (SOLAR)
TEST "H" (SKY)
(Δν)
10cm⁻¹
20
30
40cm⁻¹
50
60
70
80 cm⁻¹
90
100 cm⁻¹
110
1mm
700 μ
500
400
350
300
270
250
225
200 μ
180
160 μ
140
125
110 μ
100
90 μ
RADIATION WAVENUMBER AND WAVELENGTH

Chart III

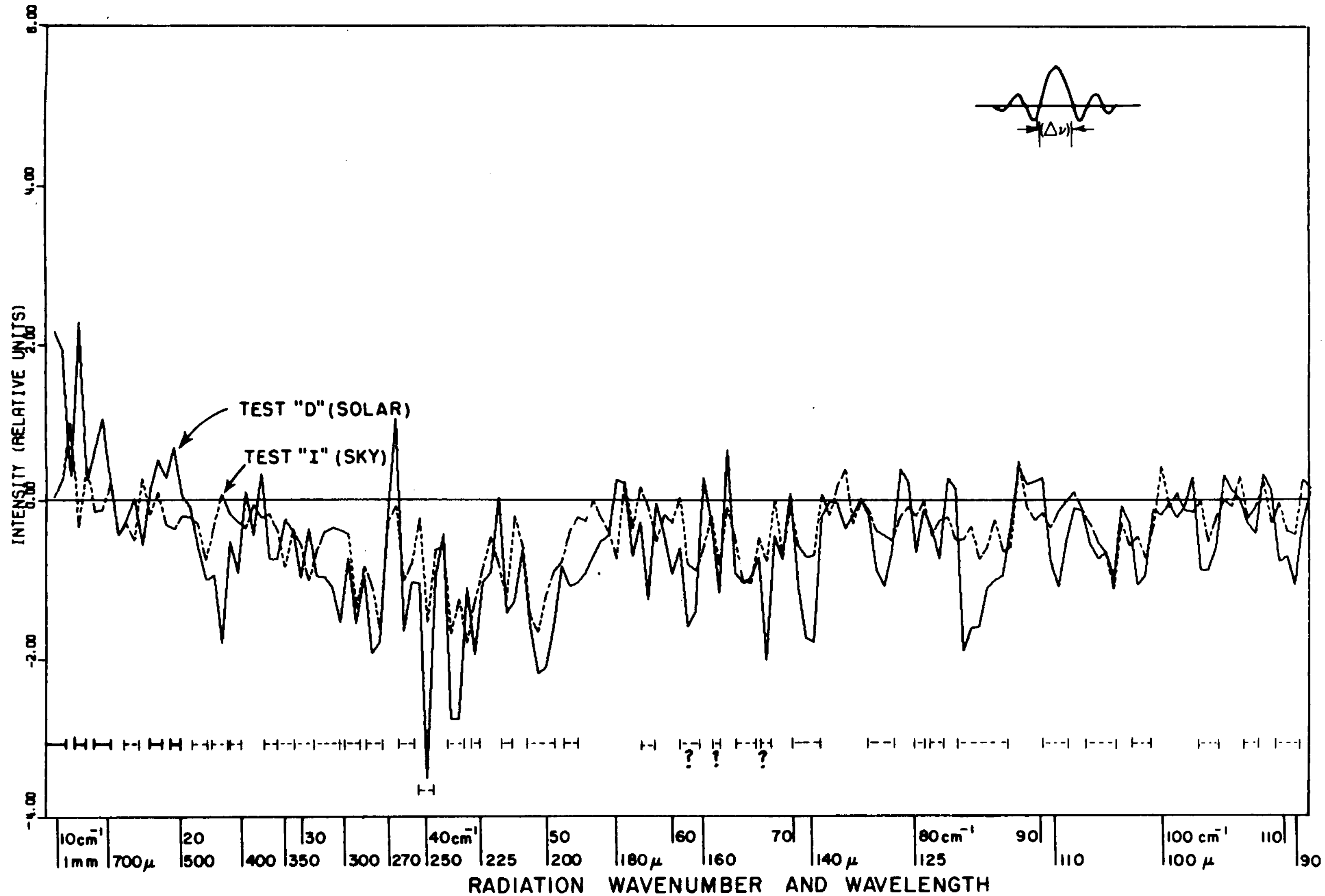
TEST "D" (SOLAR)
TEST "I" (SKY)
INTENSITY (RELATIVE UNITS)
RADIATION WAVENUMBER AND WAVELENGTH

Chart IV

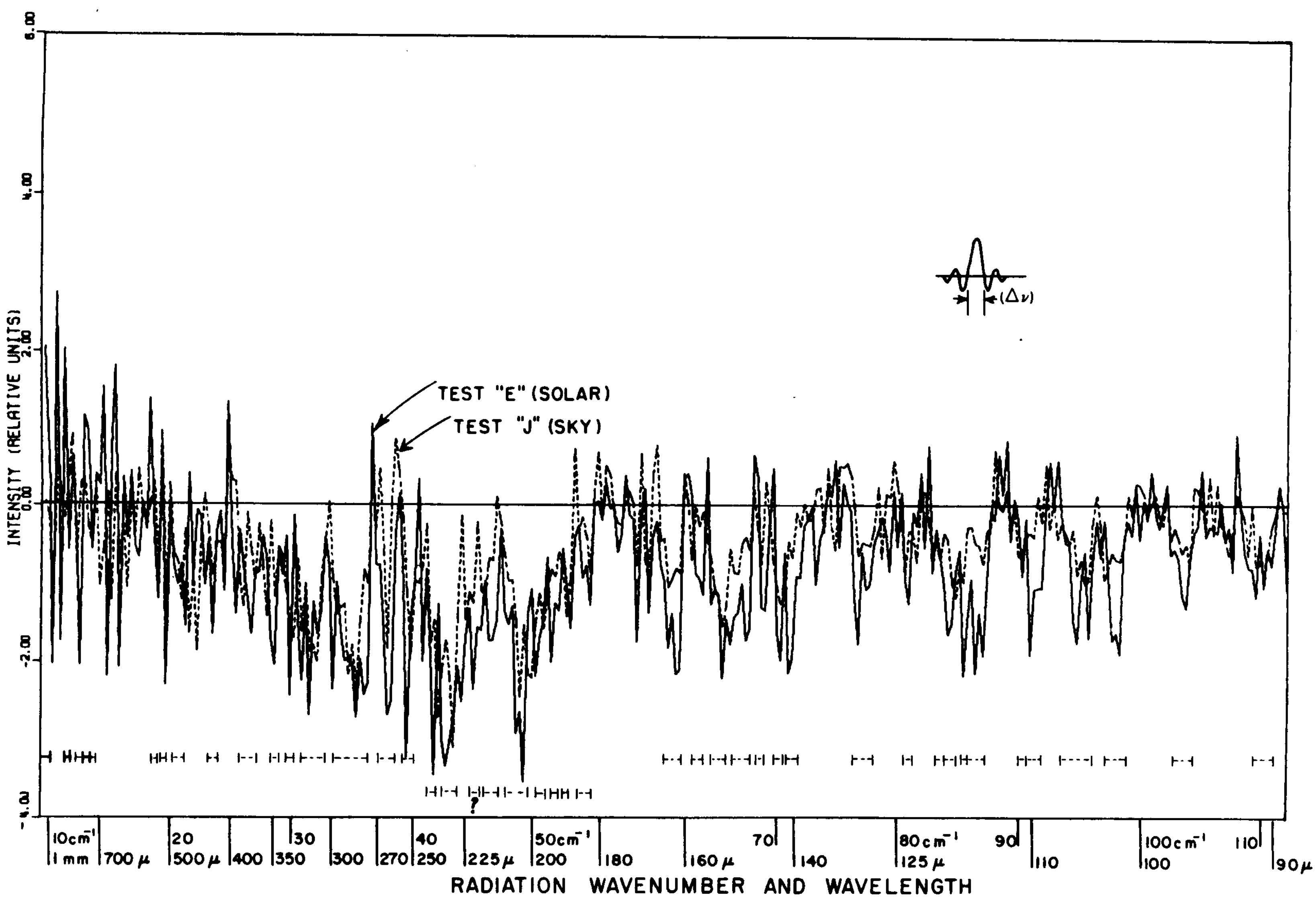

TEST "E" (SOLAR)
TEST "J" (SKY)
(Δν)
INTENSITY (RELATIVE UNITS)
6.00
4.00
2.00
0.00
-2.00
-4.00
10cm⁻¹ 1 mm
700 μ
20 500 μ
400
30 350
300
270
40 250
225 μ
50cm⁻¹ 200
180
160 μ
70
140
80 cm⁻¹ 125 μ
90
110
100 cm⁻¹ 100
110
90 μ
RADIATION WAVENUMBER AND WAVELENGTH

Chart V

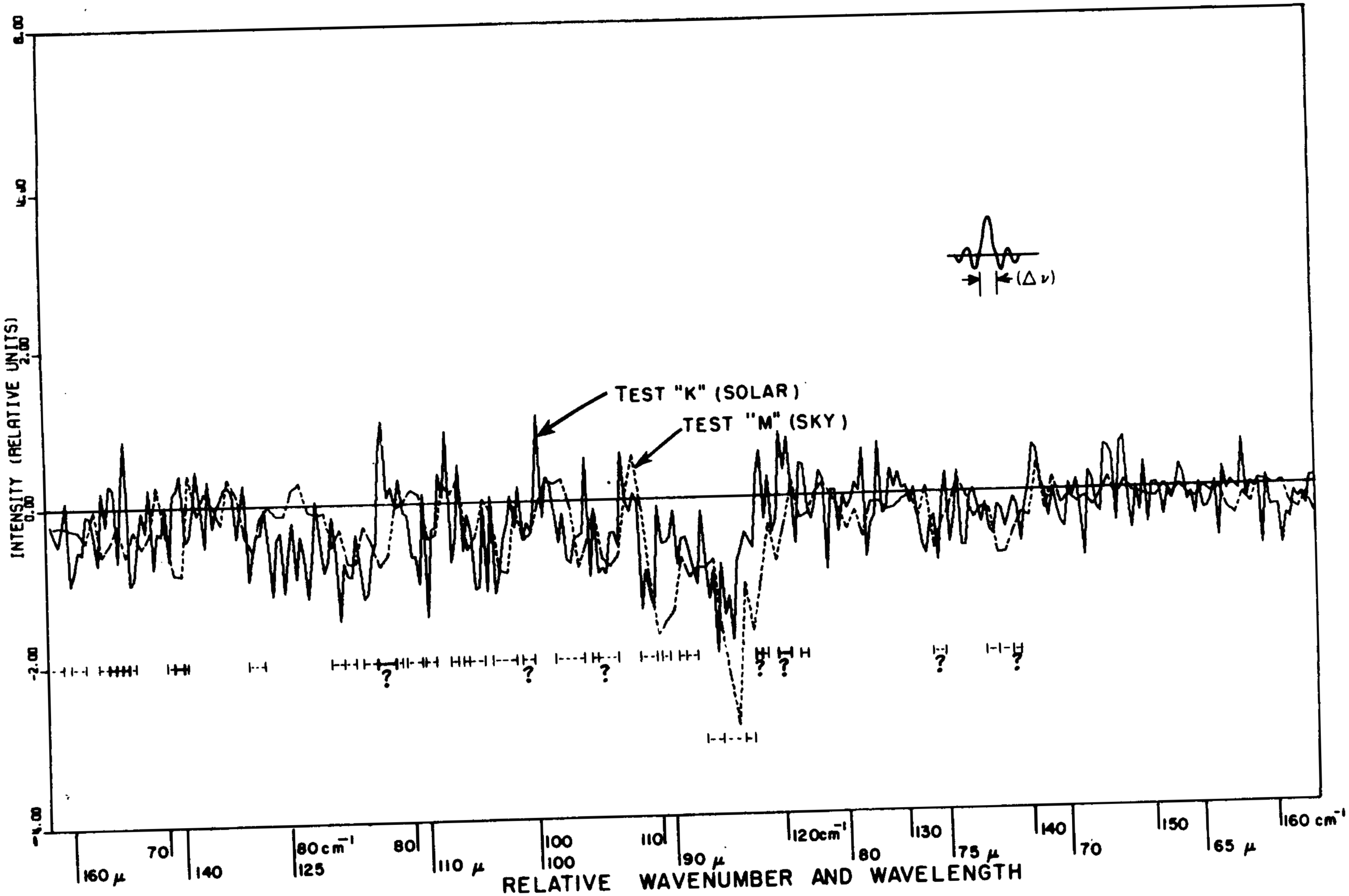

INTENSITY (RELATIVE UNITS)
TEST "K" (SOLAR)
TEST "M" (SKY)
(Δν)
RELATIVE WAVENUMBER AND WAVELENGTH

Chart VI

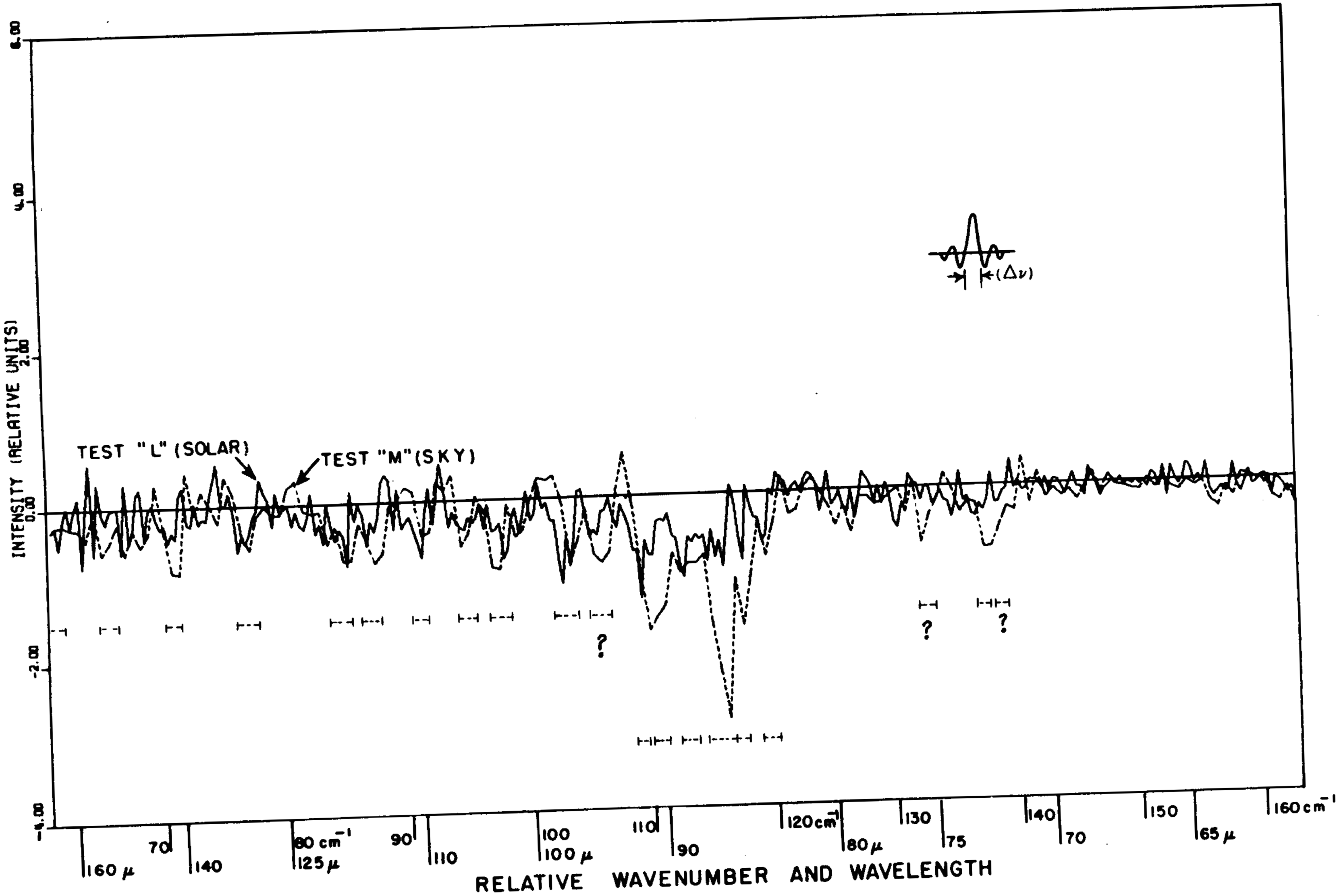
TEST "L" (SOLAR)
TEST "M" (SKY)
INTENSITY (RELATIVE UNITS)
RELATIVE WAVENUMBER AND WAVELENGTH
(Δν)
160 cm⁻¹

Chart VII

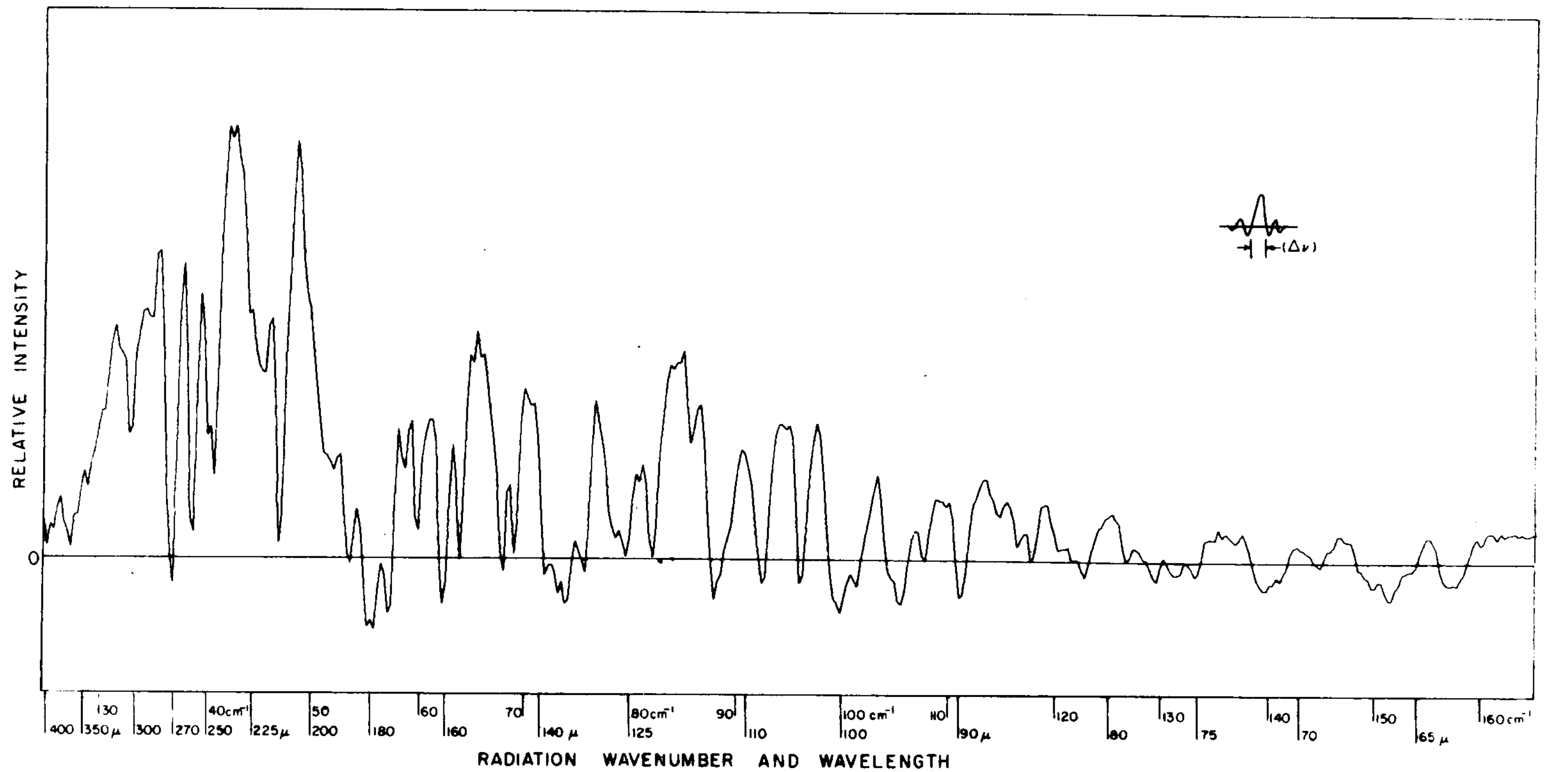

Chart VIII. Spectrum of 100°C black-body source radiation through a 2-meter path length at 17% relative humidity and 66°F.